

A tape-peeling model for spatiotemporal pattern formation by deformed adhesives

Keisuke Taga¹ and Yoshihiro Yamazaki¹

¹*Department of Physics, School of Advanced Science and Engineering,
Waseda University, Tokyo 169-8555, Japan*

(*Electronic address: tagaksk@akane.waseda.jp)

(Dated: January 30, 2023)

Abstract

We propose a new model for pattern formation in peeling of an adhesive tape based on the equation of motion for the displacement of deformed adhesives in the peel front. The spatiotemporal patterns obtained from the model are consistent with those from previous models and experiments. Moreover, dynamical and statistical properties of the patterns are investigated.

Introduction: Peeling an adhesive tape is a common daily activity, and if we look closely at the tape after peeling, we may find interesting problems in nonlinear dynamics and statistical physics. Previously one of the authors has investigated dynamical and statistical properties of spatiotemporal patterns composed of two different types of deformed adhesives in peeling [1–4]. The difference originates from whether a characteristic structure, *tunnel structure*, exists or not as shown in Figs.1 (a) and (b). It has been found that the peel speed and stiffness of the system are the main factors for controlling the formation of the spatiotemporal patterns and the formation of the tunnel structure.

Figure 1 (c) shows a typical pattern in the case of high stiffness. Peeling proceeds from top to bottom. Black and white regions show peel states without and with the tunnel structure, respectively. In the previous experimental studies, it has been known that there exists a peel speed region where a coexistence pattern such as shown in Fig.1(c) is formed. In this speed region, the following properties of the spatiotemporal patterns have been found [1, 2, 4–6]. (i) As the peel speed increases, peel state with tunnel structure becomes hard to emerge, and then the ratio of the white region decreases in the patterns. (ii) Interchange of connectivity between black and white regions occurs by changing the peel speed. (iii) Furthermore, the ratio of the white region in the coexistence pattern becomes a monotonically decreasing function of peel speed. [2, 3, 6].

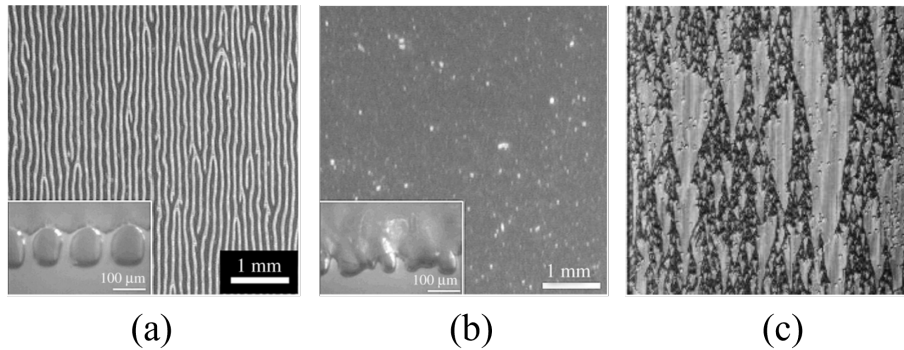


FIG. 1: Peel states (a) with and (b) without tunnel structures. Peeling proceeds from top to bottom. The small image at the bottom left in each figure shows the enlarged image of the peel front. (c) A fractal coexistence pattern. Black and white regions represent the peel states without and with the tunnel structures, respectively. The actual size of the figure is $25\text{mm} \times 25\text{mm}$.

To reproduce this pattern formation, several models have been proposed so far [2–6]. Among these models, we now comment on the model proposed in ref.[2, 5]. In this previous model, the

state variable for stability of the tunnel structure is introduced, and the peel front is considered to consist of bistable units described by the state variable. Then, the equation of motion for the peel front and the time evolution of the state variable for each unit are constructed. The asymmetric local interaction is introduced between the nearest neighbor units according to the experimental observation. This asymmetry between the units causes such an effect that once the tunnel structure collapses, then the neighboring tunnel structures tend to collapse. The previous model with the asymmetric interaction succeeds to describe the dynamics of peeling adhesive tape. However, the relation between the state transition process and the adhesive deformation process is not clear. If we consider the deformation of adhesives in peeling, we need to construct another model for adhesive deformation in the peel front.

In this letter, we propose a new model where the asymmetry of the two states is introduced not from a spatial interaction but from different local dynamics of the two peel states. Here we focus on the case of high stiffness and discuss dynamical and statistical properties of the model.

Modelling: It has been experimentally found that the peel front with the tunnel structure has larger deformation of adhesives than that without it. As in the previous model, the peel front is divided into discrete units with the size of the tunnel structure. The difference in adhesive deformation of each unit can be described by its displacement u , or $u_i(t)$ at i th unit in the peel front at time t . Large u and small u correspond to peeling with the tunnel structure and without it, respectively. Hereafter, the peel states with and without tunnel structure are referred to as the states A and B, respectively. For the time evolution of u , we consider the Newton's equation of motion and assume the phase-space dynamics illustrated in Fig. 2 is realized in the system. For the slow or fast peeling, the system has only one stable fixed point at large u or small u , which corresponds to the state A or B as shown in Figs. 2(a) and (b). And at the intermediate peel speed, the tunnel structure in the state A adjacent to the unit in the state B tends to collapse from the experiment [5], however, the tunnel structure can regenerate after a meanwhile. This dynamics seems to resemble a threshold firing dynamics and its dynamics in the phase space can be illustrated as shown in Fig. 2(c).

Based on the above consideration, the following equation is proposed for each unit:

$$\frac{d^2s}{dt^2} = -\frac{dU(u)}{du} - b\frac{ds}{dt} + \frac{a}{1+c(u-d)^2}\frac{du}{dt}, \quad (1)$$

where $s = u + Vt$ shows the length of peeled tape, and we assume $s = 0$ at $t = 0$. U is a double-well potential for bistability of the two peel states, b is viscosity of adhesives, and V corresponds to a

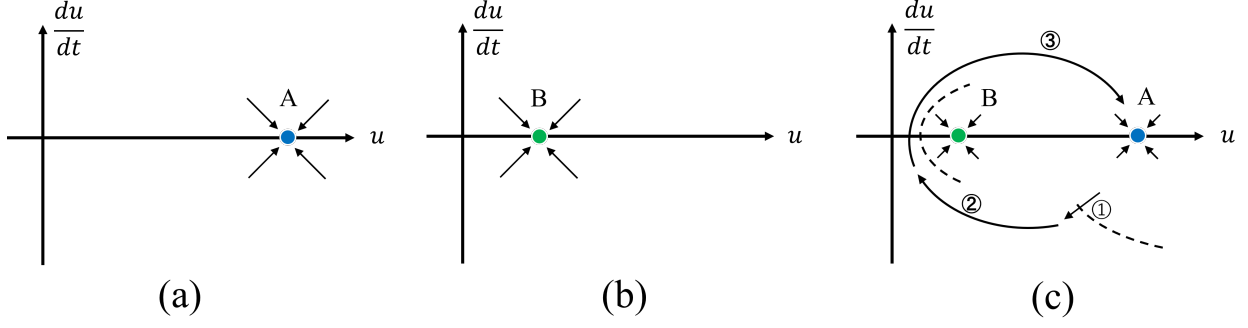


FIG. 2: Illustration of the assumed phase space dynamics.

(a) Small V . The system has only one stable fixed point as state A. (b) Large V . The system has only one stable fixed point as state B. (c) Intermediate V . The system has two stable fixed points; the states A and B. If the tunnel structure in the state A collapses with a large perturbation as ①, then the state goes to the state B as ②. And at last, the state comes back to the state A (③).

peel speed. The last term on the right-hand side shows an asymmetric dissipation, which depends on the existence of the tunnel structure. a , c and d are positive constants. For the dynamics of u instead of s , we can rewrite eq.(1) as

$$\frac{d^2u}{dt^2} = -\frac{dU(u)}{du} - b\left(V + \frac{du}{dt}\right) + \frac{a}{1+c(u-d)^2} \frac{du}{dt}. \quad (2)$$

On the right-hand side of eq.(2), the terms $-\left(\frac{dU(u)}{du} + bV\right)$ and $\left(-b + \frac{a}{1+c(u-d)^2}\right) \frac{du}{dt}$ correspond to elastic and viscous forces, respectively. Furthermore, we add the following symmetric spatial interaction terms in eq.(2):

$$D_1(u_{i+1} + u_{i-1} - 2u_i) + D_2\left(\frac{du_{i+1}}{dt} + \frac{du_{i-1}}{dt} - 2\frac{du_i}{dt}\right), \quad (3)$$

where D_1 and D_2 are positive constants. These two terms also express the effect of the viscoelasticity of adhesives.

Results: Based on eq.(2) with eq.(3), we calculated the following equation,

$$\begin{aligned} \frac{d^2u_i}{dt^2} = & -3(u_i - 1)^2(u_i - 2) - \left(V + \frac{du_i}{dt}\right) + \frac{2}{1+20(u_i - 1)^2} \frac{du_i}{dt} \\ & + (u_{i+1} + u_{i-1} - 2u_i) + 0.1\left(\frac{du_{i+1}}{dt} + \frac{du_{i-1}}{dt} - 2\frac{du_i}{dt}\right), \quad i = 1, \dots, N. \end{aligned} \quad (4)$$

$u_i = 0$ corresponds to the state where no adhesive deformation occurs. And we set $u_i \approx 2$ and ≈ 1 for the states A and B, respectively. In numerical calculation, in order to take relaxation of

adhesive deformation due to spatial inhomogeneity of adhesives into account, we reset $u_i(t) = 0$ with a probability $p = 0.001$ per unit time. As the initial condition, we set $u_i(0) = 0$ and $\frac{du_i}{dt} = 0$. Periodic boundary condition was adopted. The 4th Runge-Kutta method was used with $dt = 0.01$ in time. The discretized system size was $N = 1000$.

Figure 3 shows the typical spatiotemporal patterns obtained by the numerical calculation. The black and white regions correspond to the states B and A, respectively. There are five cases with different values of V . It is found that as V increases the ratio of white regions (the state A) decreases. And interchange of connectivity between black and white regions is confirmed. These results are consistent with those in the previous study[2].

Here the following scaling properties for the coexistent patterns are focused on: (i) the cumulative distribution $F(\geq s) \sim s^{-\xi}$ where s is the size of the white clusters, (ii) their standard deviations of the height $h(s) \sim s^{v_{\parallel}}$ and the width $w(s) \sim s^{v_{\perp}}$, and (iii) the fractal dimension D of the spatiotemporal patterns of the white regions. Our numerical results for ξ , D , v_{\parallel} , and v_{\perp} are shown in Tbl.I. For comparison, this table also has their values obtained in the previous studies [5, 6]. It is found that our present result is consistent with the previous results.

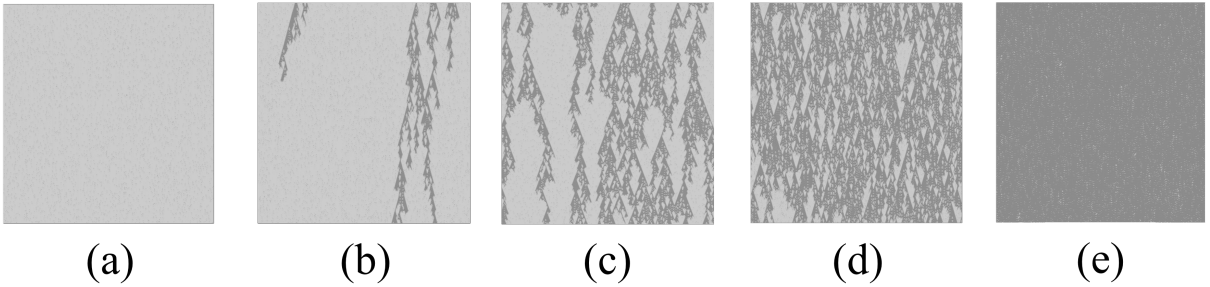


FIG. 3: Typical spatiotemporal patterns obtained by eq.(4). Time proceeds from top to bottom ($500 \leq t \leq 1200$). (a) $V = 0.29$, (b) $V = 0.30$, (c) $V = 0.309$, (d) $V = 0.32$, (e) $V = 0.50$.

Discussion: Here we comment on difference between the previous model[3] and the present model. The previous model has an asymmetric spatial interaction which expresses the situation of the state transition where the tunnel structures (in the state A) adjacent to a part of the peel front in the state B tend to collapse [5]. In the present model, we assume the local dynamics of the peel front as shown in Fig. 2 and introduce the local dissipation as a function of u instead of the previous asymmetric spatial interaction.

Figure 4 shows the nullclines and stable and unstable manifolds of eq.(4) without the spatial

TABLE I: The estimated values of the exponents.

	ξ	D	v_{\perp}	v_{\parallel}
eq.(4) at $V = 0.309$	0.78	1.82	0.63	0.45
model A at $r = 0.275$ [5]	0.85	1.70	0.58	0.41
model B at $r = 0.181$ [6]	$0.84(\pm 0.04)$	$1.61(\pm 0.01)$	$0.58(\pm 0.02)$	$0.41(\pm 0.03)$
model C at $r = 0.037$ [6]	$0.81(\pm 0.05)$	$1.62(\pm 0.01)$	$0.58(\pm 0.03)$	$0.41(\pm 0.034)$
peeling at $V = 0.48\text{mm}$ [5]	0.85	1.70	0.59	0.45

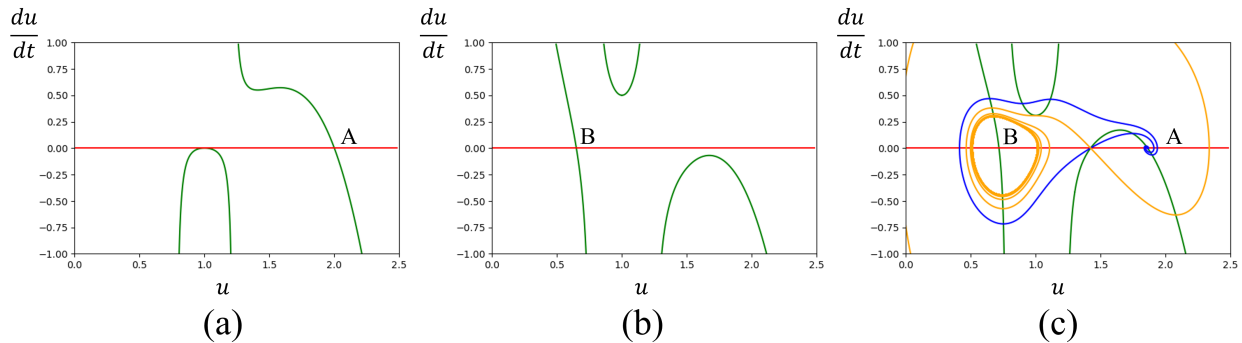


FIG. 4: Phase spaces of eq. (4) without spatial interaction. Red and Green lines are the nullcline for u and du/dt . Orange and Blue lines are stable and unstable manifolds of the saddle point. (a) $V = 0$. The system has only one fixed point as the state A. (b) $V = 0.5$. The system has only one fixed point as the state B. (c) $V = 0.309$. The system has two fixed points as the state A and B, and a threshold firing dynamics is realized.

interaction terms. For the slow or fast peeling, the system has only one stable fixed point at large $u \approx 2$ or small $u \approx 1$, which corresponds to the states A or B in Figs.4(a) and (b). And the assumed dynamics at the intermediate speed is also realized as shown in Fig. 4(c); ① if the state A crosses over the stable manifold then ② the state goes to the state B and ③ the state comes back to the state A. We consider that such a threshold firing mechanism is essential for the pattern formation of peeling adhesive tapes, although we have to experimentally verify the validity of each term in the present phenomenological model in the future.

Regarding the effect of noise, the noise term is necessary for the reproduction of the fractal spatiotemporal patterns in the previous model[3]. However, the present model does not need any noise term in the time evolution of u to reproduce the patterns as shown in Fig.3, although we

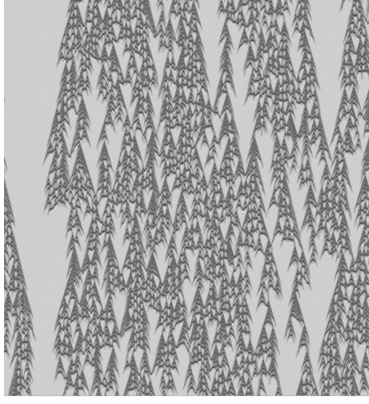


FIG. 5: A spatiotemporal pattern obtained from eq.(2) with eq.(3), $\frac{dU}{du} = 0.2(u + 0.5)(u - 1.5)(u - 4)$, $V = 0.66$, $b = 1$, $a = 1$, $c = 2$, $d = 0$, $D_1 = 1$, $D_2 = 0.1$, and $p = 0$. $500 \leq t \leq 1200$. Initial conditions of both $u_i(0)$ and $\frac{du_i}{dt}(0)$ are given with a uniform random number between -2 and 2 .

added the noise in our numerical calculation for stabilizing the state B. Actually, Fig.5 shows an example of the spatiotemporal pattern obtained from eq.(4) without noise term; we considered the randomness in u only for the initial condition. This result suggests that the fractal spatiotemporal patterns originate not from stochasticity but from chaoticity.

Finally, we note that the fractal patterns as shown in Figs.3(c) and 5 are reproducible by Bonhoffer-van der Pol type equation and other reaction-diffusion equations [7–10]. The relationship between our present model and these models can be found by transforming our model into the 2-component activator-inhibitor system as the Liénard system by introducing a new parameter $w_i \equiv \frac{du_i}{dt} + bu_i - a' \arctan(c'(u_i - d)) - D_2(u_{i+1} + u_{i-1} - 2u_i)$:

$$\frac{du_i}{dt} = -w_i - bu_i + a' \arctan(c'(u_i - d)) + D_2(u_{i+1} + u_{i-1} - 2u_i) \quad (5)$$

$$\frac{dw_i}{dt} = \left. \frac{dU}{du} \right|_{u=u_i} + bV - D_1(u_{i+1} + u_{i-1} - 2u_i), \quad (6)$$

where $a' = a/\sqrt{c}$, $c' = \sqrt{c}$. If we change the term $\frac{dU}{du} + bV$ in eq.(6) to u , then the reaction terms of eqs.(5) and (6) correspond to those of the Bonhoffer-van der Pol type equation[7]. The presence of such correspondence also suggests that the fractal patterns emerge chaotically.

Conclusion: In this letter, we have proposed a new model for pattern formation in peeling adhesive tapes which focuses on the equation of motion for the displacement of adhesives in the peel front. The model reproduces the dynamical and statistical properties of the spatiotemporal patterns which consist of the two different peel states. The previous experimental results also support our numerical results. Note that the spatiotemporal pattern obtained by the present model

is seemingly relevant to directed-percolation universality class [11]. Detailed discussions of this relevancy will be reported in near future.

-
- [1] Y. Yamazaki and A. Toda, Journal of the Physics Society Japan **71** 1618 (2002).
 - [2] Y. Yamazaki and A. Toda, Journal of the Physics Society Japan **73** 2342 (2004).
 - [3] Y. Yamazaki and A. Toda, Physica D **214** 120 (2006).
 - [4] Y. Yamazaki, K. Yamamoto, D. Kadono, and A. Toda, J. Phys. Soc. Jpn. **81** 043002 (2012).
 - [5] Y. Yamazaki, Prog. Theor. Phys. **125** 641 (2011).
 - [6] S. Ohmori and Y. Yamazaki, J. Phys. Soc. Jpn. **88** 105001 (2019).
 - [7] Y. Hayase, J. Phys. Soc. jpn. **66** 2584 (1997).
 - [8] Y. Hayase and T. Ohta, Phys. Rev. Lett. **81** 1726 (1998).
 - [9] H. Chaté, A. Pikovsky, and O. Rudzick **131** 17 (1999).
 - [10] Y. Hayase and T. Ohta **62** 5998 (2000).
 - [11] H. Hinrichsen, Adv. in Phys. **49** 815 (2000).